JOURNAL OF MATERIALS SCIENCE 14 (1979) 2887–2893

Decomposition of supersaturated solid solution in splat-cooled Sn– 10 at % Sb alloy

M. KACZOROWSKI, H. MATYJA*
*Institute of Casting, Welding and Bulk Metal Forming, and *Institute of Materials Science and Engineering, Warsaw Technical University, Narbutta 85, 02-524 Warsaw, Poland*

A supersaturated solid solution was obtained in an Sn–10 at. % Sb alloy rapidly quenched from the liquid state. Decomposition of this solution, taking place during isothermal annealing at 373 K, was investigated by transmission electron microscopy. In the first stage of decomposition, clustering of Sb atoms in definite planes of the tetragonal lattice of tin was observed. Subsequently, needle-like precipitates of the equilibrium compound SnSb were formed. The sequence of decomposition of the supersaturated solid solution Sn(Sb) and a model for the formation of the compound within the tetragonal lattice of tin are proposed.

1. Introduction

Tin-rich binary alloys with many elements of the Periodic Table were closely studied many years ago [1]. These studies were mainly concerned with the metastable phases formed in the majority of the alloys [2], as well as the variations in the solubility of alloying components and the resulting changes in lattice parameters [3]. Although the application of unconventional methods of rapid quenching [4, 5] has resulted in most systems in the formation of supersaturated solid solutions [2, 6], little attention has been given to the problem of their decomposition [7]. In those alloys in which two phases are formed from the matrix, two kinds of phase transformation in the solid state can be distinguished [8]: (1) continuous transformations involving gradual transfer from the matrix of dissolved atoms to precipitates of the second phase, and (2) discontinuous transformations, consisting in migration of the interface into the matrix; behind the interface there occurs separation into two phases with compositions different from that of the matrix. Often the attainment of the equilibrium state is preceded by the formation of metastable intermediate phases [9, 10]. The course of decomposition of supersaturated solid solutions in tin-rich alloys is of interest. In this respect the Sn–Sb system is very convenient, because it exhibits a wide solubility range varying from 10.5 at. % Sb at 519 K to about zero at room temperature [11].

2. Experimental details

A 20 g sample of Sn–10 at. % Sb alloy was made from components of 99.999% purity. Appropriate amounts of Sn and Sb were placed in a quartz ampoule under 10^{-5} Torr vacuum and melted for 1 h at 100 K above the liquidus temperature, whereupon they were quenched in water. For rapid cooling, an apparatus resembling that described by Duwez *et al.* [4] was used. Pieces of alloy weighing about 20 mg were melted in an alundum crucible at about 50 K above the melting temperature, and then they were expelled by an argon shock wave, atomized and sprayed onto a silver substrate held at the temperature of liquid nitrogen. Immediately after rapid quenching, the alloy structure was studied diffractometrically and in a transmission electron microscope.

Samples for study of the decomposition of supersaturated solid solution were placed in quartz ampoules under argon and annealed isothermally at boiling water temperature. Annealing times (τ) were 5, 10, 20, 40, 80, 160 and 320 min. The foils prepared were observed by TEM.

3. Results

Diffractometric studies were performed on a

0022–2461/79/122887–07$02.70/0

Philips PM 8000 diffractometer with the use of monochromatic Co$K\alpha$ radiation. The scanning rate was 1/120 deg sec.$^{-1}$ Immediately after rapid quenching, thin foils, together with the substrate, were placed in the goniometer holder. The silver substrate served as internal standard. The lattice parameter a of the supersaturated solid solution Sn(Sb) was calculated with the use of $h\,k\,0$ reflections, by application of the extrapolation function of Taylor and Sinclair. The parameter c was determined from six $h\,k\,l$ reflections situated at angles $2\theta > 60$ deg, separately for lines $K\alpha_1$ and $K\alpha_2$, assuming in the calculations the previously determined value of lattice parameter a. The lattice parameters thus determined are: $a = 0.582$ nm and $c = 0.3176$ nm; they only slightly differ from the values reported by Varich *et al.* [6] for this supersaturated solid solution.

The decrease in the lattice parameter c by 0.22% and the rise of parameter a by 0.36% with respect to pure tin result in a reduction of the c/a ratio. Nevertheless, the volume of the elementary cell of supersaturated solid solution is slightly increased. This was to be expected, since the atomic radius of Sb, amounting to 0.1619 nm, exceeds by 2% that of Sn [12].

The lack of reflections due to the compound SnSb indicated that as a result of rapid quenching a solid solution with 10 at.% Sb supersaturation was obtained. This conclusion was fully confirmed by electron-microscopic studies; they were performed using a Philips EM 300 transmission electron microscope fitted with a gonimeter and operating at 100 kV accelerating voltage.

Fig. 1 shows the typical structure of the alloy immediately after rapid cooling. An analysis of the electronograms and selected-area diffraction (SAD) patterns indicated that the observed foils

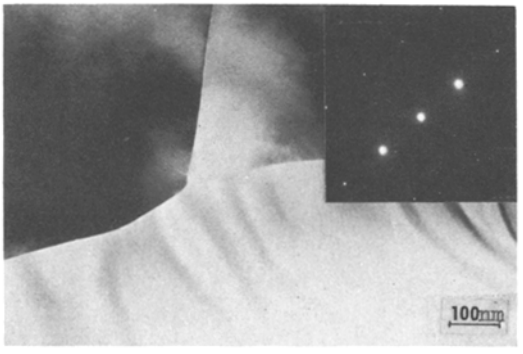

Figure 1 Microstructure of splat-cooled Sn–10 at.% Sb alloy.

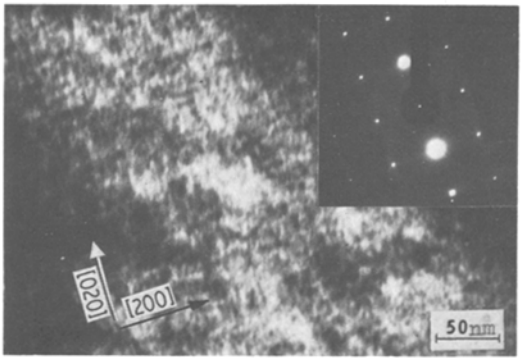

Figure 2 Bright-field micrograph of foil annealed 5 min at 373 K.

are single-phase. There were no precipitates of other phases, either of the equilibrium compound SnSb or of the metastable phases. After foil heating for 5 min at 373 K, characteristic contrasts were visible within the grains (Fig. 2). The occurrence of contrasts in electron micrographs was paralleled by the appearance of streaks in SAD patterns, which were perpendicular to vector $g = \langle 0\,2\,0 \rangle$. Marked diffusion of reflections as well as the lack of the streaks passing through reflection 0 0 0 indicated that these streaks are not due to the thin-plate shape effect; the diffuseness of reflections was rather caused by elastic strains [13, 14]. Both indications, i.e. the characteristic "substructure" observed in the electron micrograph (Fig. 2) and diffuseness in the SAD pattern, suggested that at this stage Sb atoms clustering in $\{0\,2\,0\}$ planes of the tetragonal lattice of Sn takes place. At about the same time there was migration of supersaturating vacancies, which condensed in certain regions, forming dislocation loops, as shown in Fig. 3.

Bright-field electron micrographs (Fig. 4a to d) illustrate the structure of the alloy heated for 10

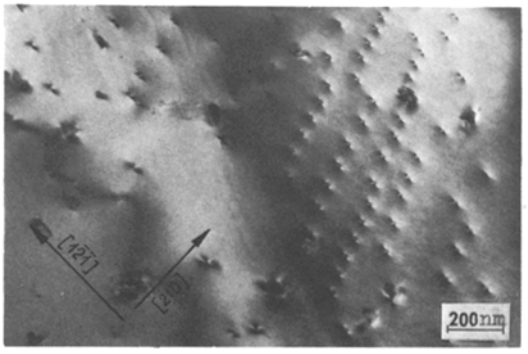

Figure 3 Dislocation loops in the same foil as in Fig. 2 after tilting of the sample.

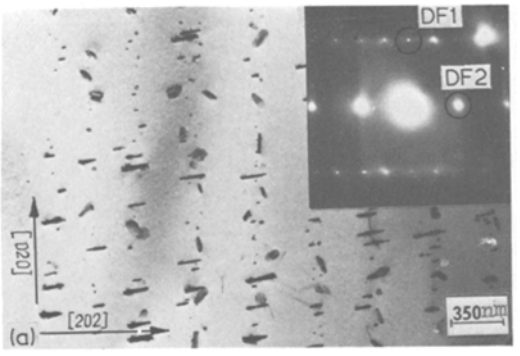

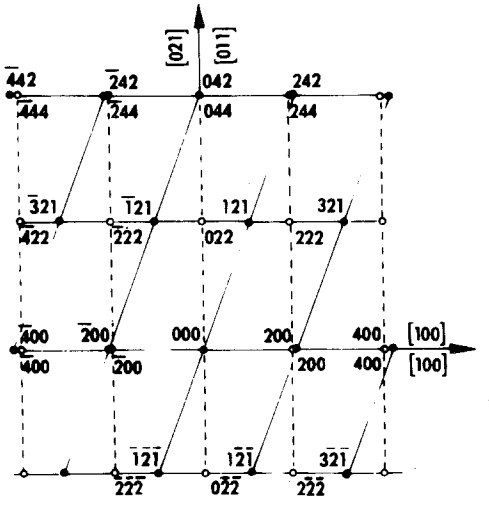

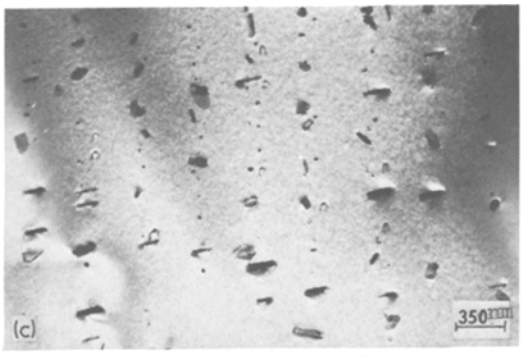

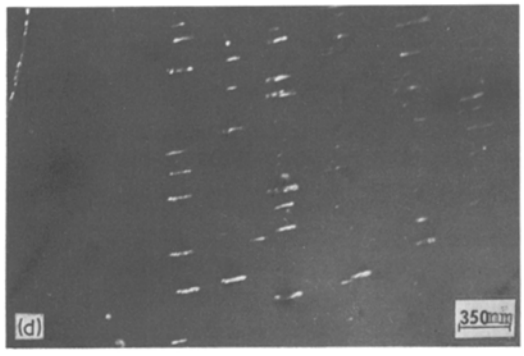

Figure 4 Microstructure of Sn–10 at.% Sb alloy annealed 10 min at 373 K: (a) TEM bright-field micrograph; (b) diagram of the electron diffraction pattern; (c) and (d) dark-field micrographs by diffracted beams from matrix and precipitates and by beams from precipitates only, respectively.

min at 373 K. Fig. 4a shows precipitates periodically distributed in the [0 2 0] direction. An analysis of the SAD pattern (Fig. 4b) indicated that precipitates of the equilibrium compound SnSb are involved. Precipitates were needle-shaped, and in most cases their length coincided with the $[2\,0\,2]_{SnSb}$ direction which was parallel to the vector perpendicular to planes of $\{2\,0\,1\}_{Sn}$ type. It is characteristic that the precipitates formed rows situated, on average, 350 nm apart, whereas the distance between precipitates in the same row was about 100 nm. It seems probable that the difference between the distance of the precipitates within a row and the distance between the rows was related to the precipitate growth direction, and presumably to the different rates of transport of Sb atoms and excess vacancies in definite crystallographic directions of the tetragonal lattice of Sn. Moreover, the periodicity of the distribution of precipitates was plainly a secondary effect of the earlier observed clustering of dissolved atoms in the {0 2 0} planes of the matrix lattice. Two further dark-field electron micrographs (Fig. 4c and d) show the same region in bright-field (Fig. 4c), and dark-field (Fig. 4d). The second electron micrograph in which bright precipitates of compound SnSb are visible, is particularly noteworthy. According to the analysis of the SAD pattern (Fig. 4b), precipitates were semi-coherent with the matrix; this is indicated by the fact that some reflections from the precipitates represented a spot system which was distinct from the matrix spot system. Analysis of many SAD patterns permitted us to establish the crystallographic relationships between the precipitate lattice and matrix lattice, which are as follows:

$$\langle 0\,2\,0\rangle_{SnSb} \| \langle 0\,2\,0\rangle_{Sn}$$

$$\{2\,0\,2\}_{SnSb} \| \{2\,0\,1\}_{Sn}.$$

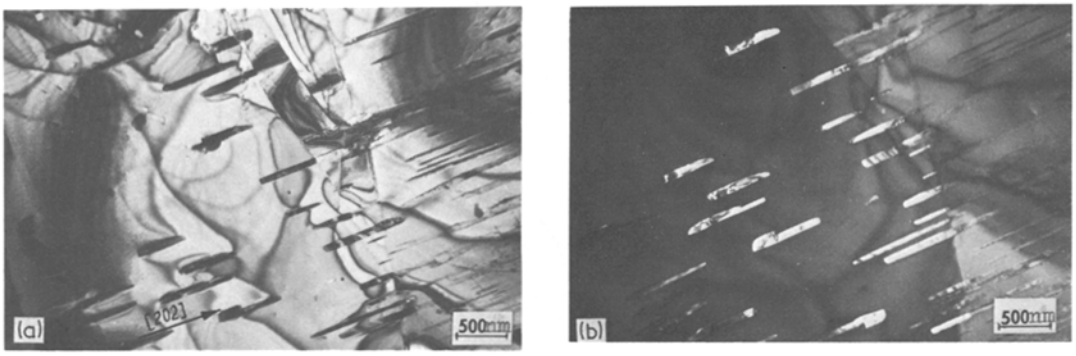

Figure 5 Microstructure of alloy after annealing for 80 min at 473 K: (a) bright-field micrograph; (b) dark-field micrograph by diffracted beams from precipitates.

The fact that the distances between {2 0 0} planes in SnSb and Sn were closely similar suggested coherence between the precipitates and matrix along just these planes. This was confirmed by SAD patterns in which $g = \langle 0\,2\,0\rangle^{SnSb} \| g = \langle 0\,2\,0\rangle^{Sn}$. Moreover, coherence in these planes led to the occurrence of elastic strains caused by misfit between $d^{SnSb}_{0\,2\,0}$ and $d^{Sn}_{0\,2\,0}$; this explains the diffuseness of reflections in the directions perpendicular to vector $g = \langle 0\,2\,0\rangle$, as observed in the SAD pattern shown in corner of Fig. 4a.

Two bright- and dark-field electron micrographs (Fig. 5a and b) show the structures of alloy after heating for 80 min at 373 K. In the dark-field electron micrographs, the growth of the precipitates in the $[2\,0\,2]_{SnSb}$ direction was clearly visible.

Successive stages of the growth of precipitates of the equilibrium compound SnSb are shown in Fig. 6a and b. Fig. 6a presents the precipitates in the form of thick needles distributed in the [2 0 1] and [0 2 1] directions of the matrix. The mean length of the precipitates was about 2 μm and their thickness was 0.1 to 0.2 μm. This structure was obtained after foil annealing for 160 min at boiling water temperature. Double the length of foil heating at the same temperature led to further growth of the precipitates which became more rounded. The change in shape was doubtless due to the tendency for reduction of surface energy of the precipitates, and thus to a decrease in total free energy of the system. Long-term annealing of the foil produced compound SnSb precipitates in the form of tetrahedrons analogous to those which occur in Sn–Sb alloys prepared by conventional casting.

4. Discussion

Diffraction and electron microscopic studies show that rapid quenching of the Sn–10 at.% Sb alloy from the liquid state results in an extension of the solubility range to 10 at.% Sb, this being constistent with earlier reports [6]. After alloy annealing for 5 min at 373 K, the decomposition of supersaturated solid solutions begins; it consists in clustering of Sb atoms in {0 2 0} planes of the

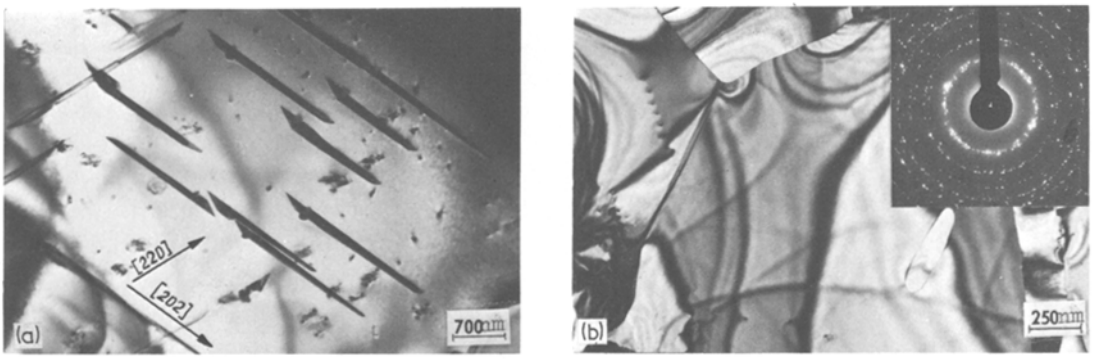

Figure 6 Growth of the precipitates in specimen annealed at 473 K: (a) for 160 min; (b) for 320 min.

matrix. As a result, a periodic substructure similar to that obtained during spinodal decomposition is formed [15]. After further annealing there is formation of precipitates of equilibrium compound SnSb, which may not yet have the Sn:Sb stoichiometric ratio of 1:1, but which shows a SnSb structure similar to the regular structure of NaCl-type. (The equilibrium compound SnSb has a rhombohedral structure with angle $\alpha = 89.5°$, in which atoms are distributed similarly as in the elementary cell of NaCl.) These precipitates grow in the form of needles and are semi-coherent with the matrix. The elongated shape of precipitates is consistent with the theory of phase transformations in the solid state, which predicts that coherent or semi-coherent precipitates are plate- or needle-like, in contrast to non-coherent precipitates most often assuming the shape of spheroidites or tetrahedrons. It is of interest that the decomposition of the supersaturated solid solution Sn(Sb) is not preceded by formation of a metastable intermediate phase, as observed for other alloys [16] and as is expected from Ostwald's rule [17], but takes place directly. Direct precipitation of SnSb compound is most likely related to the great similarity in the lattice parameters between a double cell of tetragonal tin obtained by superimposing two elementary cells, and the elementary cell of compound SnSb. Let us assume for simplification that compound SnSb shows a regular structure of type B3 ($\alpha = 89.5° \approx 90°$). In this case for Sn, $a = 0.5831$ nm and $2c = 0.6364$ nm, whereas the lattice parameter of compound SnSb is: $a = 0.6138$ nm (ASTM: 4-0673 and 1-0830). Structure B3 can readily be obtained by slight shift of the atoms in directions [0 0 1] and [0 0 $\bar{1}$] within the cell formed by superposition of two cells of tetragonal Sn. The state before and after the atom shift is shown in Fig. 7a and b, in which the directions of shifts of the individual atoms are denoted by arrows. The proposed model is confirmed by the earlier established crystallographic relationships between the precipitate lattice and matrix lattice.

If it is assumed that Ostwald's rule applies to all systems, then the absence of metastable intermediate phases during the decomposition of supersaturated solution Sn(Sb) can be explained by the relatively low stability of this solution (the decomposition is completed at room temperature after a few days). The annealing temperature of 373 K, applied in these studies, is fairly high and amounts to $0.7\,T_m^*$. It seems quite reasonable to assume that in this case the annealing temperature T_A is much higher than the hypothetical critical temperature T_c which is the highest temperature at which the supersaturated solid solution could decompose with formation of metastable intermediate phases. The schema of the above considerations is shown in Fig. 8, illustrating the hypothetical course of the changes in free enthalpies of the different phases as a function of temperature.

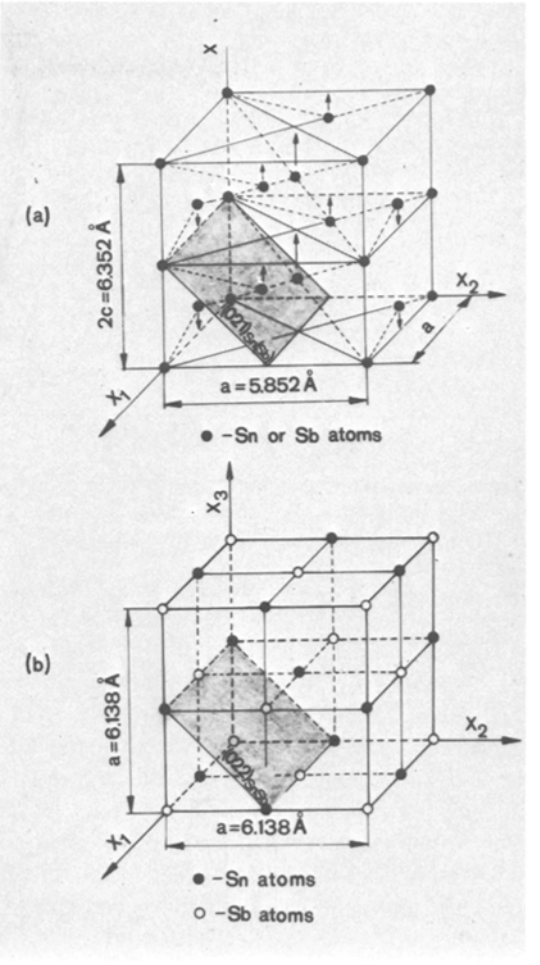

Figure 7 Schematic diagram of unit cells showing: (a) supersaturated Sn(Sb) solid solution before shifting of the atoms; (b) SnSb compound after shifting and full reordering of the atoms in double Sn unit cells.

The formation of SnSb is doubtless promoted

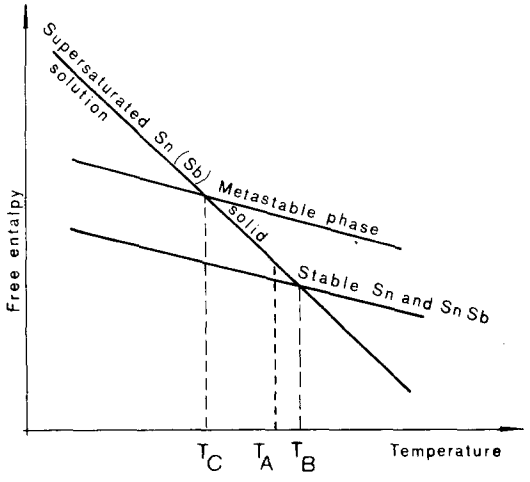

Figure 8 Schematic hypothetical free enthalpy/temperature diagram representing the possible decomposition reactions of supersaturated solid solution Sn(Sb).

by the occurrence of this compound within a certain concentration range, which – consistent with the equilibrium diagram – can exist at a content of 42 to 58 at.% Sb. On account of the considerable supersaturation as well as of the presence of supersaturating vacancies retained in the alloy after rapid quenching, direct formation of SnSb nuclei and, subsequently, their growth seem to be quite possible. In view of the reduction of the number of precipitates, their further growth probably proceeds via coagulation, consisting of the absorption of smaller precipitates by the larger ones.

According to the above considerations, the sequence of the decomposition of supersaturated solid solution obtained in rapidly quenched alloy Sn–10 at.% Sb can be set out as in Fig. 9.

5. Conclusions

(1) As a result of rapid quenching of the Sn–10 at.% Sb alloy from the liquid state, supersaturated solid solution Sn(Sb), with tetragonal structure and lattice parameters $a = 0.5852$ nm and $c = 0.3176$ nm, is obtained.

(2) Decomposition of the supersaturated solid solution at 373 K is of the nature of a continuous reaction and proceeds according to the schema presented in Fig. 9. Namely, at the first stage of decomposition, clustering of Sb atoms in planes {2 0 0} of the tetragonal lattice of Sn takes place. Subsequently, needle-like precipitates of compound SnSb are formed; they are semi-coherent with the matrix and grow mainly in directions $\langle 2\,2\,0\rangle_{SnSb}$. The elongated shape of the precipitates is consistent with the predictions of the theory of phase transformations in solid state.

(3) The lack of any metastable intermediate phases (which consistent with Ostwald's rule often precede the formation of equilibrium phases) can be explained by: (a) relatively high annealing temperature ($T_A = 0.71\,T_m$); (b) similarity in the lattice parameters between the double cell of tetragonal Sn and elementary cell of compound SnSb; (c) ease of formation of the lattice

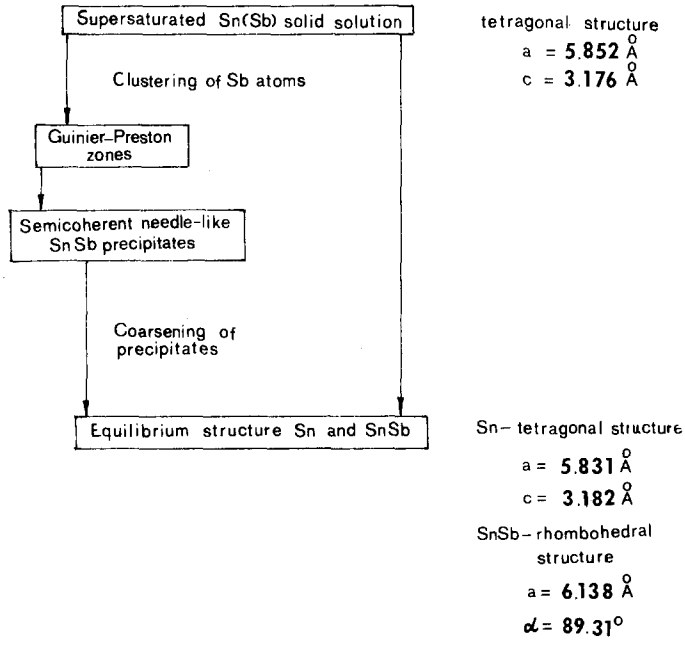

Figure 9 Schematic diagram of decomposition of super-saturated Sn(Sb) solid solution annealed at 373 K.

of compound SnSb by a slight atom shift in directions [0 0 1] and [0 0 $\bar{1}$] within the cell formed by superposition of two cells of tetragonal Sn, and (d) facilitated diffusion caused by the presence of supersaturating vacancies, which permits obtainment of a sufficiently high Sb atom concentration necessary for nucleation of equilibrium compound SnSb.

Acknowledgement

The authors thank B. Dąbrowski for helpful comments and discussion and Dr I. Jampoler for her help with translation of this paper.

References

1. G. V. RAYNOR and J. A. LEE, *Acta Met.* **2** (1954) 616.
2. R. H. KANE, B. C. GIESSEN and N. J. GRANT, *ibid* **14** (1966) 605.
3. J. A. LEE and G. V. RAYNOR, *Proc. Phys. Soc.* **LXVII, 10-B** (1954) 737.
4. P. DUWEZ and R. H. WILLENS, *Trans. AIME* **227** (1963) 362.
5. G. FALKENHAGEN and W. HOFFMAN, *Z. Metallk.* **43** (1952) 69.
6. N. I. VARICH and A. A. JAKUNIN, *Izv. Akad. Nauk USSR Metally* **2** (1968) 229.
7. S. K. KHERA, P. K. K. NAYAR, Proceedings of the Symposium on Materials Science Research, NAL, Bangalor, India, 11 Feburary, (1970) p. 345.
8. J. W. CHRISTIAN, in "The Theory of Transformations in Metals and Alloys" (Pergamon Press, Oxford, 1965) ch. 1.
9. M. H. JACOBS, A. G. DOGGETT and M. J. STOWELL, *Fizika 2 suppl. 2* paper 18 (1970).
10. M. KACZOROWSKI, J. KOZUBOWSKI, B. DĄBROWSKI and H. MATYJA, *J. Mater. Sci.* **13** (1978) 407.
11. M. HANSEN, in "Constitution of Binary Alloys" (McGraw-Hill, New York, 1958) p. 1175.
12. W. KLEVER, in "An Introduction to Crystallography" (Veb Verlag Technik, Berlin, 1970) p. 152.
13. P. B. HIRSCH, A. HOWIE, R. B. NICHOLSON, D. W. PASHLEY and M. J. WHELAN in "Electron Microscopy of Thin Crystals" (Butterworths, London, 1965) ch. 6, 14.
14. G. THOMAS, in "Modern Diffraction and Imaging Techniques in Material Science" (North-Holland, Amsterdam, 1970) p. 131.
15. R. M. FISHER and J. D. EMBURY, in "Electron Microscopy 1964" Vol. A. (Chech. Academy of Science, Prague, 1964) p. 149.
16. M. KACZOROWSKI, J. KOZUBOWSKI, B. DĄBROWSKI, H. MATYJA, *J. Mater. Sci.* **13** (1978) 1105.
17. L. S. DARKEN and R. W. GURRY "Physical Chemistry of Metals" (McGraw-Hill, New York, 1953).

Received 10 October and accepted 1 November 1978.